

## Electronic Supplementary Information

### **Asymmetric bead aggregation for microfluidic immunodetection**

Sunggu Kim, Sanghoon Han, and Junghoon Lee\*

*Department of Mechanical and Aerospace Engineering, Seoul National University,*

*1, Gwanak-ro, Gwanak-gu, Seoul 08826, South Korea*

\*To whom correspondence should be addressed

E-mail address: [jleenano@snu.ac.kr](mailto:jleenano@snu.ac.kr)

## S1. The trajectory of the AIB inside the microchannel while reaching the surface

As an AIB moves in the middle of the microchannel, it is subjected to the magnetic force, drag force, and gravitation force. When  $x$  and  $z$  are the distance of the AIB from the center of the cylindrical magnet, the forces of the  $x$  and  $z$  components acting are determined as <sup>1-3</sup>

$$F_{AIB,x}(t) = F_{mag,x}(x, z) - F_{drag,x}(t) \quad (1)$$

$$F_{AIB,z}(t) = F_{mag,z}(x, z) - F_{drag,z}(t) - F_g \quad (2)$$

Where

$$F_{mag,x}(x, z) = \mu_0 V \chi M_s^2 R_{mag}^4 \frac{x}{2[x^2 + z^2]^3} \quad (3)$$

$$F_{mag,z}(x, z) = \mu_0 V \chi M_s^2 R_{mag}^4 \frac{z}{2[x^2 + z^2]^3} \quad (4)$$

And

$$F_{drag,x} = 6\pi\eta R_{AIB}(v_{AIB,x}(t) - v_f(z^*)) \quad (5)$$

$$F_{drag,z} = 6\pi\eta R_{AIB} v_{AIB,z}(t) \quad (6)$$

Where

$$z^* = z - R_{mag} \quad (7)$$

$$v_f(z^*) = \frac{3\bar{v}_f}{2} \left[ 1 - \left( \frac{h_c - z^*}{h_c} \right)^2 \right] \quad (8)$$

(All constants are given in table S1)

While the AIB is moving, the magnetic force becomes equal to the drag force and gravitation (buoyance) force;

$F_{AIB,x}(t) = F_{AIB,z}(t) = 0$ . Thus, the position of the AIB ( $x'$ ,  $z'$ ) at time  $T$  is determined by

$$x'(T) = x'(0) + \int_0^T v_{AIB,x}(t) dt = x'(0) + \int_0^T \left[ \frac{\mu_0 V \chi M_s^2 R_{mag}^4}{6\pi\eta R_{AIB}} \left( \frac{x_m - x'(t)}{2[(x_m - x'(t))^2 + (z_m - z'(t))^2]^3} \right) + v_f(z'(t)) \right] dt \quad (9)$$

$$z'(T) = z'(0) + \int_0^T v_{AIB,z}(t) dt = z'(0) + \int_0^T \left[ \frac{\mu_0 V \chi M_s^2 R_{mag}^4}{6\pi\eta R_{AIB}} \left( \frac{z_m - z'(t)}{2[(x_m - x'(t))^2 + (z_m - z'(t))^2]^3} - F_g \right) \right] dt \quad (10)$$

Where  $x_m$  and  $z_m$  are the distance from the center of the magnet to the edge of the starting point (10 mm and 5 mm respectively) and ( $x'$ ,  $z'$ ) is the position from the bottom edge of the microchannel (see Fig S1b). By applying numerical analysis using iterative calculation, the trajectory of AIB in the flow is estimated as Fig S1d (Initial conditions:  $x'(0) = 0$ ,  $z'(0) = 37.5 \mu\text{m}$ ,  $v_{AIB,x}(0) = 333 \mu\text{m/s}$ ,  $v_{AIB,z}(0) = 0$ ). It takes approximately 19 seconds for the AIB to reach the microchannel surface and 5.4 mm in the horizontal direction (single-bonded AIB). In most cases, AIBs successfully reach the top surface before entering the sensing area and are ready to slide. Likewise, trajectory of PS and MG beads can be estimated. A PS, on the other hand, moves almost along the sample flow due to lack of magnetism while a MG quickly reaches the surface. Figure S1 shows the detailed dimensions and magnetic field applied to the microchannel. The cylindrical magnet is diametrically magnetized and is oriented along the  $x$ -axis. The numerical estimation was performed using MATLAB (R2016b, Mathwork<sup>®</sup>). With the help of the calculations, we optimized the placement of the magnet and sensing area so that most of the AIBs are able to slide in the sensing area properly.

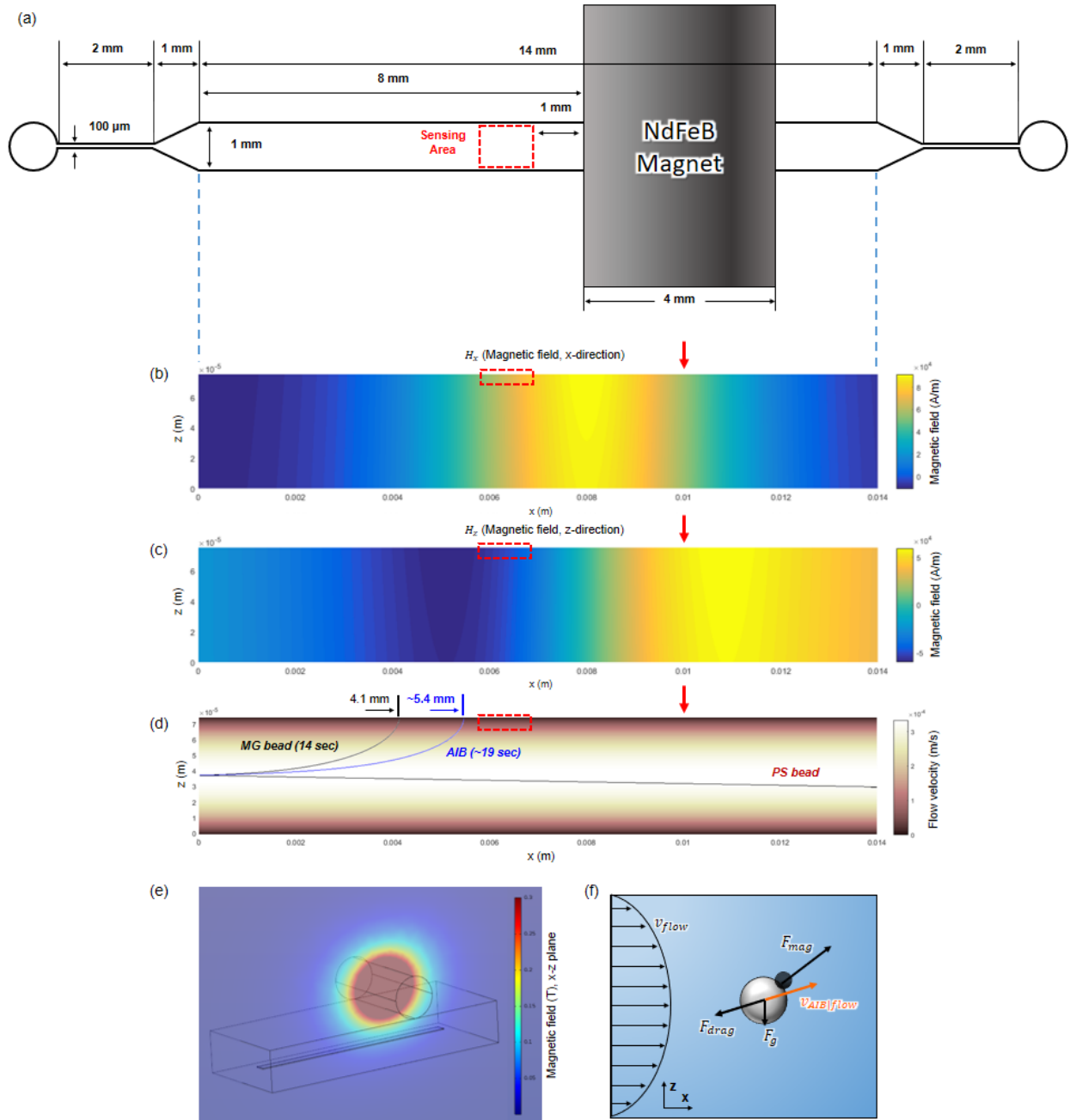


**Fig. S1** (a) Detailed dimensions of the microfluidic channel and position of the cylindrical magnet (top view). (b) The x-component and (c) z-component of the estimated magnetic field inside the microchannel (cross-sectional view). (d) Velocity profile of the flow and estimated trajectory of each bead (MG, AIB, and PS). Red dotted boxes indicate the sensing area and red arrow indicates the center of the magnet. (e) Simulation of the magnetic field of the device (COMSOL Multiphysics 5.2), (f) Various forces exerted on the AIB during the rise. The drag force is proportional to the relative velocity between the AIB and the sample flow. Gravitational force is no longer negligible when AIB is placed far away from the magnet.

**Table. S1** Constants and variables

$v_{AIB}(t)$	Velocity of the AIB at time $t$
$v_f(z)$	Sample flow velocity at height $z$ in the microchannel
$m_{AIB}$	Mass of the AIB ( $1.29 \times 10^{-14}$ kg)
$F_g$	Gravitation force – Buoyance force ( $7.8 \times 10^{-15}$ N)
$\mu_0$	Magnetic permeability constant ( $1.26 \times 10^{-6}$ N/A <sup>2</sup> )
$V$	Volume of MG (Dynabead Myone bead, $6.06 \times 10^{-19}$ m <sup>3</sup> )
$\eta$	Viscosity of water ( $1.0 \times 10^{-3}$ N s/m <sup>2</sup> )
$\chi$	Effective magnetic susceptibility of MG (Dynabead Myone bead, 0.3)
$M_s$	Magnetized level of the cylindrical NdFeB magnet ( $1.11 \times 10^6$ A/m)
$R_{mag}$	Radius of the magnet (2 mm)
$R_{AIB}$	Effective radius of the AIB (1.42 $\mu$ m)
$\bar{v}_f$	Average velocity of the sample flow (222 $\mu$ m/s)
$h_c$	Half of the height of the microchannel (37.5 $\mu$ m)

## S2. Velocity reduction of sliding AIB in the sensing area.

As the AIB slides along the flow and gets closer to the magnet, the magnetic force becomes stronger. Therefore, the net force in the x-direction induced by the external magnetic field also changes. The magnetic force and the friction force applied to the AIB are estimated as shown in Fig S2. Specifically, the net force ( $F_{mag,x} - \mu_k F_{mag,z}$ ) in the x-direction is -0.04 pN on average in the sensing area and smallest at the outermost edge. For single-bond AIB, the velocity is reduced by 3.6% across the sensing area. Similarly, the velocity reduction in 2PS-MG AIB is 2.1% and in the PS-2MG AIB is 6.7%. Thus, the sliding velocity in the sensing area hardly changes by the magnetic force.

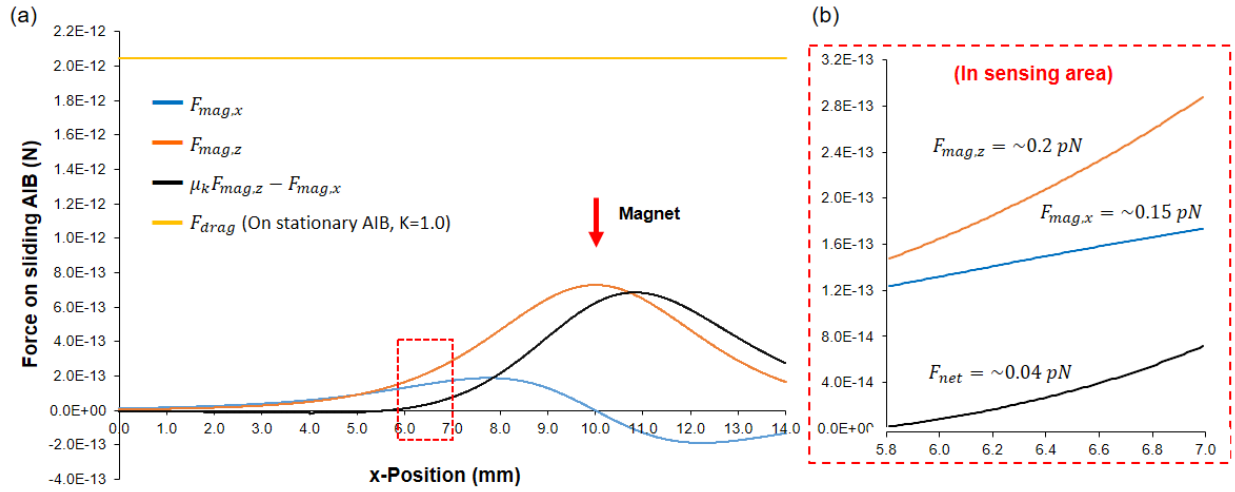


Fig. S2 (a) The magnetic force and friction force on sliding AIB throughout the microchannel (The magnet is placed at  $x = 10$  mm). (b) The magnetic force inside the sensing area. The net force induced by the external magnet is about -0.04 pN in x-direction when the friction coefficient is 0.85 ( $\mu_k = 0.7 \sim 1.0$ ).

### **Video S1. Various types of AIBs and their relative sliding velocities**

The relative sliding velocity of each type of AIB is presented as an example.

### **Video S2. Sliding behavior of AIBs at various NP concentrations**

A short video shows a difference in sliding behavior of each sample during measurement; five different NP concentrations.

### **References**

1. E. P. Furlani and K. C. Ng, *Physical Review E*, 2006, **73**, 061919.
2. F. Liu, P. Kc, G. Zhang and J. Zhe, *Analytical Chemistry*, 2016, **88**, 711-717.
3. M. A. M. Gijs, F. Lacharme and U. Lehmann, *Chemical Reviews*, 2010, **110**, 1518-1563.